Temperature, composition, and hydrogen isotope effect in the hydrogenation of CO on amorphous ice surface at 10–20 K

H. Hidaka, A. Kouchi, and N. Watanabe[a)]
Institute of Low Temperature Science, Hokkaido University, Sapporo 060-0819, Japan

(Received 12 December 2006; accepted 5 April 2007; published online 25 May 2007)

An experiment on the addition reaction of a D atom (deuteration) to CO on a cold ice surface is performed by deuterium atom exposure of three types of samples (pure solid CO, CO-capped H_2O ice, and CO–H_2O mixed ice) at 10–20 K. The variation of IR absorption spectra for the samples was measured by a Fourier transform infrared spectrometer during exposure to deuterium atoms. Reactions on pure solid CO were observed only at 10 K, while reactions on CO-capped H_2O ice and CO–H_2O mixed ice were observed to proceed even at 20 K. This indicates that the coexistence of H_2O at the surface raises the reactive temperature. In addition, the experiment on H atom exposure was also carried out at 15 K to compare the reaction rate constant between the H and D atoms. The ratio of reaction rate constant k_D/k_H obtained is about 0.08 at 15 K. The authors provide information on the potential energy for the H+CO reaction at the surface by using the ratio k_D/k_H and by a model calculation of the potential tunneling with the asymmetric Eckart potential. © *2007 American Institute of Physics*. [DOI: 10.1063/1.2735573]

I. INTRODUCTION

Although thermally activated chemical reactions are suppressed at cryogenic temperatures, chemical reactions involving light particles such as hydrogen atoms, often proceed due to the quantum mechanical tunneling effect or the so-called tunneling reaction. The tunneling reaction is a good case study for quantum mechanics and is of great interest for physical chemists. Furthermore, tunneling reactions are key processes for chemical evolution in the very cold regions, such as molecular clouds of space. Although tunneling reactions can proceed much faster than thermally activated reactions at very low temperatures, the tunneling reactions of atoms and molecules are still significantly slow to be measured in the typical duration of gas phase experiments. Therefore, tunneling reactions have often been studied in the solid phase wherein the reactants stay nearby and thus easily interact with each other for long times; the reactions can therefore be observed within the experimental duration. For example, there have been several experiments on the reaction of atomic hydrogen using electron spin resonance. Kumada *et al.*[1] estimated the tunneling rate constants for the reaction $HD+D \rightarrow H+D_2$ in solid HD at 2.6–6.5 K. The isotope effect on the production and decay of H and D atoms in γ radiolysis of solid D_2–H_2 mixtures was studied at 4 K.[2] Miyazaki *et al.* reported the temperature effect on the decay of H(D) atoms for the radiolysis of solid H_2, D_2, and HD at 4.2 and 1.9 K.[3] For tunneling reactions of the hydrogen molecule, Hoshina *et al.* determined the reaction rates for $R+H_2 \rightarrow RH+H$ ($R=CD_3, CD_2H, CDH_2, CH_3$) reactions in solid parahydrogen at 5 K by Fourier transform infrared spectroscopy (FTIR).[4] In addition, measurements of the rate constant of the hydrogen abstraction reaction, $CH_3+CH_3CN \rightarrow CH_4+CH_2CN$, by tunneling were performed in the temperature range of 77–125 K.[5] In these experiments, the solid samples themselves were used as one of the reactants. In contrast, there are only a limited number of studies for atom-molecule or molecule-molecule tunneling reactions between adsorbates on solid surfaces. These are commonly expected for the processes on interstellar grains.

In the present paper, we focus on the addition of hydrogen atoms to CO molecules (hydrogenation) on the surface of amorphous H_2O ice at very low temperatures. The hydrogenation of CO is particularly important in astrochemistry because both H_2O and CO are primordial molecules in molecular clouds and have been observed abundantly on interstellar grains.[6] Theoretical studies have suggested that the successive hydrogenation of CO via tunneling reactions on grain surfaces would be the main route for the production of formaldehyde (H_2CO) and methanol (CH_3OH).[7] Hiraoka *et al.* attempted to confirm this process by experiments using H atoms sprayed on to solid CO.[8] However, since they did not measure the flux or fluence of atoms, quantitative information such as reaction rates could not be extracted from the IR results. Recently, we performed a series of experiments on the hydrogenation of CO on various solid surfaces in the temperature range of 8–20 K, which revealed that H_2CO and CH_3OH can be produced by the successive hydrogenation of CO (Refs. 9–12) by tunneling in an astronomical environment.

$$CO + H \xrightarrow{k_H} HCO, \tag{1}$$

$$HCO + H \rightarrow H_2CO, \tag{2}$$

$$H_2CO + H \rightarrow CH_3O \text{ or } CH_2OH, \tag{3}$$

a)Electronic mail: watanabe@lowtem.hokudai.ac.jp

$$CH_3O + H \rightarrow CH_3OH. \quad (4)$$

The activation energy of reaction (1) has been reported to be several thousands of kelvins by several groups.[13–17] The reported activation energies are scattered over a wide range and are only for gas phase reactions. The reactions at the solid surface differ from those in the gas phase because of the different potential energy surfaces. In fact, Xie *et al.* demonstrated theoretically that an atom-molecule reaction $^{13}O+HC_3N$ can be effectively catalyzed by water ice to be barrierless.[18] Furthermore, the reaction rates must depend on the composition and structure of the surface.[12] The determination of both the activation energy of the hydrogenation of CO and the reactivity at the various surfaces are essential to an understanding of the chemical evolution on interstellar grains. Here, we report the study of an isotope effect on the addition reaction of hydrogen atoms to CO and the dependence of the reactivity on the surface composition at several temperatures. The isotope effect on the reaction rate is a good probe in investigating the potential surface of the reaction because the tunneling reaction strongly depends on the particle mass. The ratio of reaction rate constants k_D/k_H is derived by the experimental results of D and H atom addition reactions to CO on an amorphous H_2O surface at 15 K.

II. EXPERIMENT

The apparatus used in the study, apparatus for surface reaction in Astrophysics (ASURA), and the experimental procedure used have been described previously.[12,19,20] Briefly, three types of solid samples, pure solid CO, CO–H_2O mixed ice, and CO on H_2O ice (CO-capped H_2O ice) were prepared at 10–20 K. The samples were formed on a cold aluminum substrate by vapor deposition through a capillary plate in an ultrahigh vacuum chamber (ca. base pressure of 10^{-8} Pa). The sample area was surrounded by a copper shroud that was connected to a liquid nitrogen reservoir to enhance the pumping speed for H_2O. The compositions of the samples were measured by FTIR with a resolution of 1 cm^{-1}. The sample thickness was calculated from the column density divided by the surface density on the assumption of a bilayer of solid ice for a surface density of 10^{15} molecules cm^{-2}. In our setup, the column density is given by following equation:

$$N = \frac{\cos\theta}{2A}\int \zeta d\zeta, \quad (5)$$

where N is the column density (molecules cm^{-2}), θ is the IR incident angle, A is the integrated absorption coefficient (molecules cm^{-1}), and ζ is the absorbance. The incident angle is about 83°, and the integrated absorption coefficients are 1.1×10^{-17} molecules cm^{-1} for the C–O stretching of CO (Ref. 21) and 2.0×10^{-16} molecules cm^{-1} for the O–H stretching of H_2O.[22] The thickness of pure solid CO was about 2 ML. The CO–H_2O mixed ice was prepared in the same manner as that described in the previous report.[10] The thickness of the mixed ice was about 20 ML with an H_2O/CO ratio of 4. The CO-capped H_2O ice consisted of about 0.8 ML of CO at the top and underlying 10 ML. Statistical uncertainties in the thicknesses were within 10%. Since the surface structure of the deposited amorphous H_2O ice is normally very rough, the concept of a monolayer may differ from the usual idea of a closely packed layer.

The hydrogen and deuterium atoms were produced by a microwave-induced plasma in a Pyrex tube and transferred through an aluminum pipe to the ice sample. The aluminum pipe was connected to the cold head of a He refrigerator. The recombination of H(D) atoms on the aluminum surface is suppressed at low temperatures.[23] In the present experiment, the atomic hydrogen and deuterium were cooled by passing them through the cold aluminum pipe at 50 K, as measured by an AuFe 0.07%–Chromel thermocouple attached to the aluminum pipe at the downstream end. However, since the atoms from the pipe must be spread widely, some portion of the atoms will be way off the sample and will collide with the liquid nitrogen shroud. These atoms may gain an energy of about 100 K at the surface of the shroud and subsequently impinge on the sample. Thus, the temperature of the atoms would not be perfectly 50 K but will be distributed within 50–100 K. No photons were detected from the plasma when a photodiode was inserted in front of the substrate. A deflector was mounted at the end of the aluminum pipe. This transfer system for the atoms achieves not only the acquisition of a low energy atomic beam but also the removal of charged particles and long-lived-metastable H(D) atoms from the plasma.

The H and D atoms were monitored by a quadrupole mass spectrometer (q mass) with a Faraday cup. The q mass head was located just behind the substrate on the opposite side of the atom source. For the flux measurements, the cold head with the substrate was moved down such that the q mass was in sight of the atom source. The increase in the intensities, namely, the q-mass readings (ΔQ_H and ΔQ_D), for H (mass 1) and D (mass 2) atoms were measured when the microwave discharge was turned on. Since the measurement with the q mass does not directly yield the flux, we converted ΔQ_H to the equivalent increase in pressure ΔP_H to determine the flux (f_H) of the H atoms. In other words, we determined the proportional factor a in the relation

$$\Delta P_H = a\Delta Q_H. \quad (6)$$

The factor a is independent of the gas species used. Once the factor a was obtained, the f_H could be calculated by the following relationship:

$$f_H = \frac{c_H \Delta P_H \langle v\rangle}{4k_B T} = \frac{c_H a \Delta Q_H \langle v\rangle}{4k_B T}, \quad (7)$$

where c_H is the calibration factor of the pressure gauge for H atoms, k_B is the Boltzmann constant, $\langle v\rangle$ is the mean velocity of H at 100 K, and T is the atom temperature. Since the H beam contains a significant amount of undissociated H_2, we could not measure the exact value of ΔP_H even for atomic beam operation. Therefore, H_2 gas was used instead to obtain a. H_2 gas was filled in the chamber from a variable leak valve on the top flange and was measured by the q mass and the cold cathode gauge (MKS HPS903). Using this setup, we obtained $a=1.12\times10^5$ Pa/A. In this measurement, the pressure was set to be close to that during the atomic beam operation. Finally, it is to be noted that the fluxes of H and D

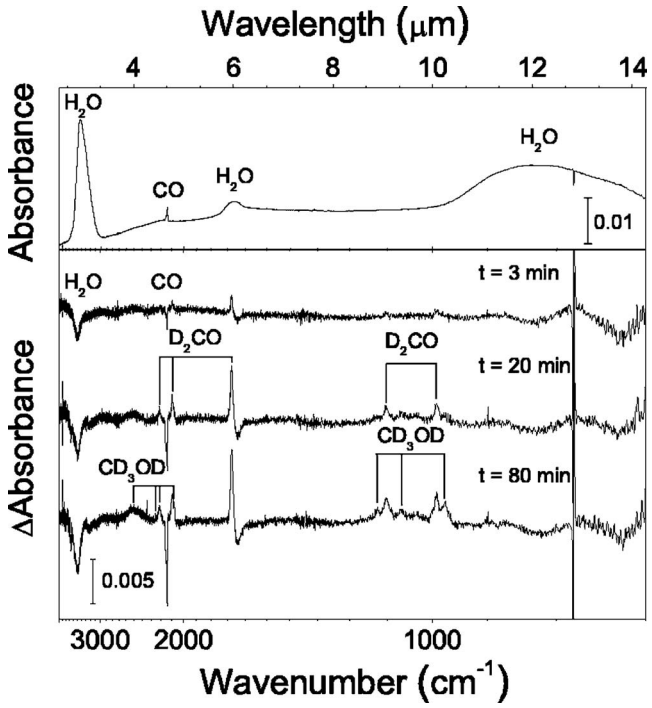

FIG. 1. IR absorption spectrum of initial CO-capped H_2O ice (*top*) and variation of the absorption spectra (*bottom*) with D atom exposures of 3, 20, and 80 min. The spectra were obtained by subtracting the initial (*nonexposed*) absorption spectra from the spectra after D atom exposure. Peaks below and above the base line represent decreases and increases in the absorbance, respectively. The *x*-axis scale is set for the reciprocal wave number. The spikes at around 780 cm^{-1} in all the spectra represent noise.

atoms were both 2.6×10^{14} cm^{-2} s^{-1} in the present experiment. The atomic beam was monitored before and after exposure of the sample ice. The stability of the beam fluxes were good.

III. RESULTS AND DISCUSSION

Figure 1 shows the variation in the IR absorption spectra of CO-capped H_2O ice at 15 K during exposure to deuterium atoms. These spectra clearly indicate the formation of D_2CO and CD_3OD when the samples were exposed to deuterium atoms. For the short exposure time, several new peaks arise at around 991, 1103, 1677, 2098, and 2212 cm^{-1} with a decrease in CO at 2142 cm^{-1}. These peaks are assigned to the D_2CO vibration mode of CD_2 wagging, CD_2 scissoring, CO stretching, CD stretching, and CD_2 scissoring over tone,[24] respectively. As the exposure time increases, additional new peaks appear at 977, 1067, 1126, 2078, 2250, and 2430–2450 cm^{-1} (broad peak), corresponding to the CD_3OD vibration mode of CO stretching, CD_3 asymmetry bending, CD_3 symmetry bending, CD_3 symmetry stretching, CD_3 asymmetry stretching, and OD stretching,[25] respectively. Although CD_3OD has one more CD_3 asymmetry stretching mode at around 2217 cm^{-1}, we cannot distinguish that from the broad peak of the CD_2 scissoring overtone (2212 cm^{-1}) in D_2CO. In addition, these peak patterns of D_2CO and CD_3OD were confirmed to be consistent with the IR spectra of pure solid D_2CO and CD_3OD samples in our setup. For both the pure solid CO and CO–H_2O mixed ice, peak patterns of D_2CO and CD_3OD were also obtained and no additional peaks were observed. When the exposure was stopped, no further change was observed in the spectra. This indicates that the formation reactions occurred immediately after exposure.

The prominent absorption peaks of the DCO radical have been reported at 1937 and 1926 cm^{-1} in a CO (Ref. 26) and argon matrix,[27] respectively. Although the peak position of DCO is expected to shift in our sample because of the different composition of the matrix, no peak was observed in the wide range (1850–1950 cm^{-1}) in our spectra. The absorption peaks for the CD_2OD radical appear at 1221–1238 cm^{-1} in the N_2 (Ref. 28) and Ar (Ref. 29) matrices at 14 K; however, no peak was observed at 1150–1300 cm^{-1} in the present experiment. Unfortunately, the peak positions of the CD_3O radical in the low temperature matrix have not been previously reported. In the gas phase, the fundamental CO stretching of the ground state CD_3O was reported at 1010 cm^{-1}.[30] Since no peaks appear around 1010 cm^{-1} and all the peaks in our spectra are assigned, we conclude that the CD_3O radical is not detected. We also experimentally checked whether the reactions of $CO+D_2\rightarrow D_2CO$ and $D_2CO+D_2\rightarrow CD_3OD$ occurred, since undissociated D_2 molecules are present in our atomic beam. When the samples were exposed to D_2 molecules alone, no reactions occurred. It is not clear in the present experiment whether the intermediate radical reactions with the D_2 molecule, i.e., $DCO+D_2\rightarrow D_2CO+D$ and CD_3O (CD_2OD) $+D_2\rightarrow CD_3OD+D$, occurred. However, in the hydrogen system, $HCO+H_2\rightarrow H_2CO+H$ and $CH_2OH+H_2\rightarrow CH_3OH+H$ reactions are endothermic by +40 kJ/mol (Ref. 14) and +33 kJ/mol,[31] respectively. Although the reaction $CH_3O+H_2\rightarrow CH_3OH+H$ is slightly exothermic (−1 kJ/mol), the calculated activation barrier of this reaction is over 6000 K in the gas phase.[31] Thus, the methanol formation process of CH_3O+H_2 is less likely than the barrier-free formation process of CH_3O+H. Since the differences in the zero-point energy between the H and D systems in these endothermic reactions are much smaller than the heats of the reactions, the energetic relations would not change in the case of the deuterated radical and D_2 reactions. Therefore, we believe that these deuterated radical reactions with D_2 are negligible.

The reaction paths to the observed products are considered to be the same as those for the production of CH_3OH by hydrogenation in previous experiments.[9–11] That is, the following reactions:

$$CO + D \xrightarrow{k_D} DCO, \tag{8}$$

$$DCO + D \rightarrow D_2CO, \tag{9}$$

$$D_2CO + D \rightarrow CD_3O \text{ or } CD_2OD, \tag{10}$$

$$CD_3O + D \rightarrow CD_3OD, \tag{11}$$

where k_D is a reaction rate constant of reaction (8). The failure to detect radicals indicates that the reaction rate constants

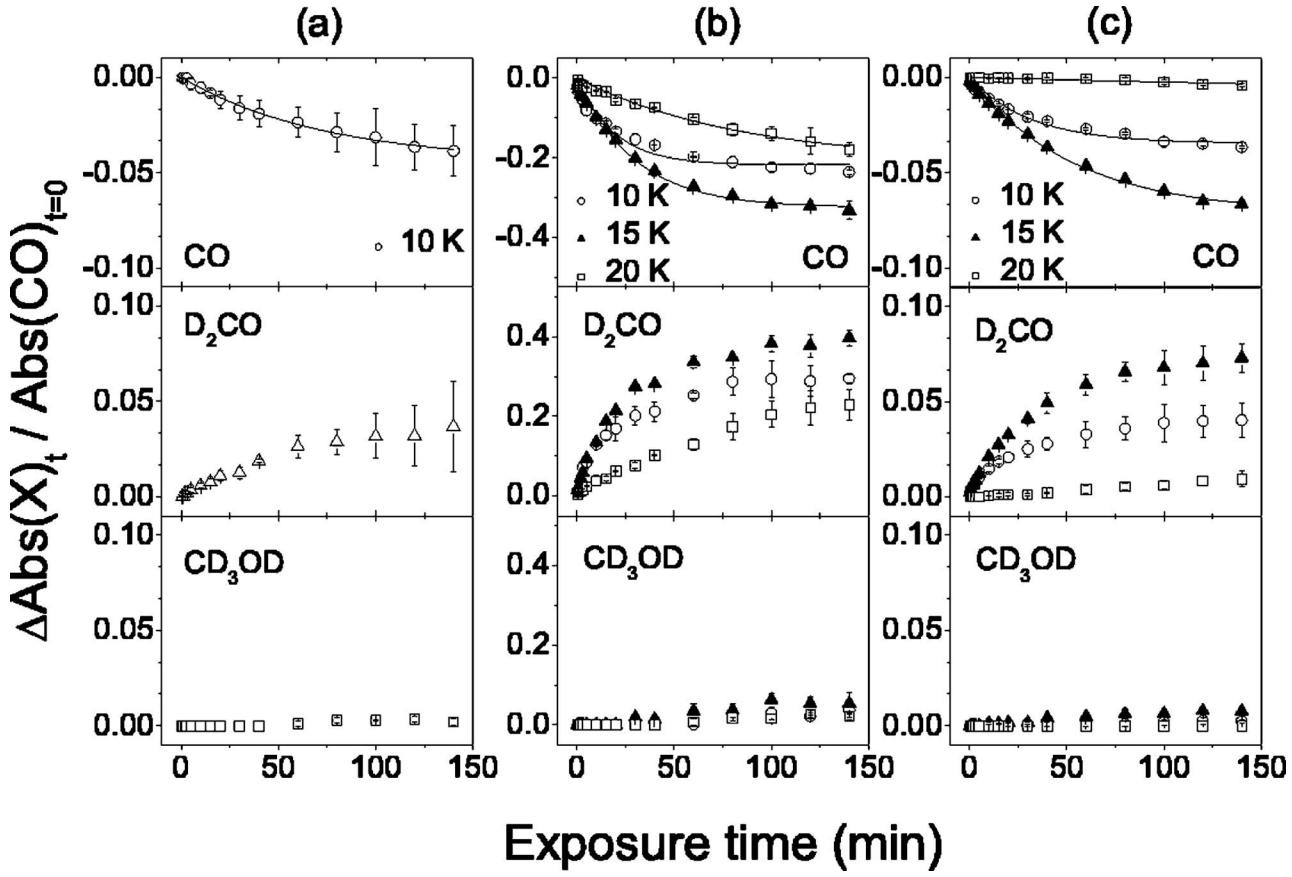

FIG. 2. The variation in absorbance of CO (*top panels*), D_2CO (*middle panels*), and CD_3OD (*bottom panels*) as a function of exposure time at 10–20 K. (a) Pure solid CO; (b) CO-capped H_2O ice; (c) CO–H_2O mixed ice. The absorbances are normalized by that of the initial CO. Error bars represent the statistical errors. The solid lines represent the least-squares fitting of the CO decay curves to a single exponential function Eq. (12).

of reactions (8) and (10) are much smaller than those of reactions (9) and (11), respectively.

In the present experiment, the large flux must induce D–D recombination reactions producing the heat of the reaction (about 431.3 kJ/mol) on the solid sample. Part of this heat of reaction would be released to the sample surface. If the recombination reaction causes local heating at the surface, crystallization of the amorphous ice and desorption of the adsorbed molecules should be induced because the activation energies of these processes are near 100 K which is much less than the heat of reaction. The phase change of ice and the desorption of molecules can both be monitored by the change in the IR absorption spectra. It is well known that the peak shape of the OH-stretching band is different between crystalline and amorphous ice.[22] If the parent or product molecules are desorbed, the peaks of these molecules should monotonically decrease. No such evidence was observed in the present experiment. Therefore, we concluded that local heating did not occur and that the D–D recombination did not affect the deuteration of CO. The heat of reaction due to recombination would be carried away partly by the internal and translational energies of the D_2 molecule produced and would partly diffuse immediately into the bulk.

Figure 2 shows the variations in the integrated absorbance of CO (2142 cm^{-1}), D_2CO (1677 cm^{-1}), and CD_3OD (977 cm^{-1}) bands on the D atom exposure of samples at 10–20 K as a function of exposure time. The vertical axis is normalized by the integrated absorbance of the initial CO. The reactivities for all the samples drastically changed within the narrow temperature range of 10–20 K. This implies that the deuterium atoms reacted with CO after adsorption on the surface, the so-called Langmuir-Hinshelwood or hot atom processes. If the reaction occurs via the Eley-Rideal process, that is, if atoms from the gas phase collide directly and react with the adsorbed reactants, the reactivity must depend on the incident energy of the atoms rather than the surface temperature. However, we found in the previous experiments[9] that the dependence of reactivity on the incident energy of atoms is much weaker than that on the surface temperature in the incident energy range of 80–300 K. Hornekær *et al.* performed experiments on the exposure of amorphous H_2O ice to H and D atoms with fluxes of $\leqslant 10^{13}$ at. cm^{-2} s^{-1} at 8 K.[32] They observed fast recombination to produce H_2 and D_2, indicating short diffusion times before encountering each other. Since our atom flux (2.6×10^{14} at. cm^{-2} s^{-1}) is about one order of magnitude higher than that used by Hornekær *et al.*, the incident atoms must immediately encounter the CO molecules on the surface. In our experimental condition, the reaction rates would not be restricted by the surface diffusion of atoms but by the tunneling rates of the potential for the addition reactions. Consequently, the CO decay curves can be fitted by

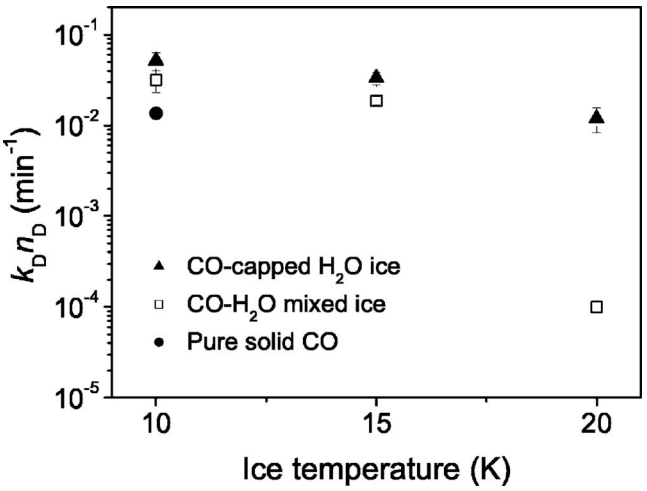

FIG. 3. Plots of the effective rate constants for CO+D reaction on pure solid CO (*solid circle*), CO-capped H_2O ice (*solid triangles*), and CO–H_2O mixed ice (*open squares*). $k_D n_D$ values are obtained by fitting the data to Eq. (12).

$$\frac{[\Delta CO]_t}{[CO]_0} = -\epsilon\{\exp(-k_i n_i t) - 1\} \quad (i = \text{H or D}), \tag{12}$$

where ϵ is a saturation value, t is the exposure time, and n_i and k_i are the number density of atoms on the surface and the reaction rate constant for H and D atoms, respectively. Unfortunately, the reaction rate constant k_i cannot be separated from the fitting parameter of $k_i n_i$ because it is very difficult to estimate the absolute value of n_i. Here, we assume that n_i is time independent and is governed mainly by the balance between the flux of the atoms, the sticking coefficient of the impinging atoms, and the loss of atoms by H(D)–H(D) recombination. Since the activation energy of the recombination reaction, namely, radical-radical reaction, must be much lower than those of the reactions with molecules such as CO, the losses of atoms by reaction with molecules such as CO are negligible. The value of $k_i n_i$ is defined as the effective rate constant. Figure 3 represents the temperature dependence of the effective rate constant $k_D n_D$ for D atom addition to CO determined by the fitting of the CO-depletion data to Eq. (12).

All effective rate constants decrease with increasing ice temperature. Since chemical reaction is normally promoted by an increase of the temperature for the thermally activated reactions or is temperature independent for tunneling reactions, this temperature dependence is considered to be due to a decrease in the sticking coefficient of the D atoms with increasing temperature. In the case of pure solid CO, the addition reaction was observed only at 10 K and no change was observed above 15 K on exposure. On the other hand, the addition reaction for CO-capped H_2O ice and CO–H_2O mixed ice proceeds up to 20 K [Figs. 2(b) and 2(c)]. This wider range of the reactive temperature due to the existence of H_2O was also observed in the previous experiments.[12,20] We ascribe this to the higher sticking coefficients of atoms to H_2O ice compared to the sticking coefficients to pure solid CO. The results for pure solid CO implies that D atoms barely stick to the sample surface above 15 K as discussed in Ref. 12 In the H_2O-contained samples, a large number of H_2O molecules are exposed at the top of the surface. Thus, the incident atoms can first be adsorbed on the H_2O ice and react with neighboring CO molecules even above 15 K. Above 20 K, reactions were barely observed even for the H_2O-contained samples. Many experiments have also demonstrated that the reaction efficiency for chemical reactions involving hydrogen atoms on the H_2O ice surface decreases as the ice temperature approaches 20 K.[32,33] This strongly suggests that the sticking coefficient of hydrogen atoms to H_2O ice decreases significantly near 20 K. Alternatively, H_2O ice would work like a catalyst as suggested by Xie *et al.*[18]

For CO-capped H_2O and CO–H_2O mixed ice samples, the D atom addition reaction to CO was almost saturated for an exposure of 140 min at 10 and 15 K, and the saturation values increased with temperature as shown in Fig. 2. This temperature dependence of the saturation value would be attributable to the different diffusion lengths of the D atom in the different temperatures. In our previous work on H +CO–H_2O mixed ice, the difference in the saturation value was quite small between 10 and 15 K.[10] This is due to the easier diffusion of H atoms having a lower mass than the D atoms. As can be seen in Fig. 3, the effective rate constants of the reaction, D+CO, in mixed ice is smaller than that for the capped ice for all ice temperatures, although both are two component systems of CO and H_2O. We attribute the difference in the effective rate constant to CO coverage on the ice surfaces. The CO coverage must be different for the CO-capped H_2O and the CO–H_2O mixed ice. The reaction was not observed on pure solid CO at 15 K. Pure solid CO can be regarded as unity CO coverage. That is, the effective rate constant decreases with an increase in the CO coverage at the ice surface, because the average sticking coefficient to the entire area of the surface becomes smaller; in other words, the number density of the adsorbed D atoms on the surface becomes smaller. In order to investigate the effect of CO coverage on the effective rate constant, we performed D atom exposure of CO-capped H_2O ice samples to various amounts of CO at 15 K. The CO decay curves thus obtained, which are not shown, were fitted using Eq. (12) to estimate the effective rate constants. The effective rate constants $k_D n_D$ are plotted in Fig. 4 as a function of the amount of adsorbed CO on H_2O ice at 15 K. $k_D n_D$ clearly decreases with increasing amount of CO. In Fig. 4, the CO coverage for the surface of CO–H_2O mixed ice at 15 K corresponds to that of about 1.1 ML CO-capped H_2O ice.

The ratio of the reaction rate constants for CO+D $\rightarrow$DCO and CO+H$\rightarrow$HCO is of major interest for this study. In order to compare the rate constant of CO+D to that of CO+H, we performed an experiment of H atom exposure of CO (0.8 ML)-capped H_2O ice at 15 K with the same atom flux as the D atom beam. Figure 5 shows CO depletion curves for CO+D$\rightarrow$DCO and CO+H$\rightarrow$HCO reactions at 15 K. The effective rate constants $k_D n_D$ and $k_H n_H$ obtained by fitting to Eq. (12) are 0.033 and 0.41 min^{-1}, respectively. To determine the ratio of the rate constants k_D/k_H, the ratio of n_D/n_H is required.

As described above, n_H (n_D) would be governed by the

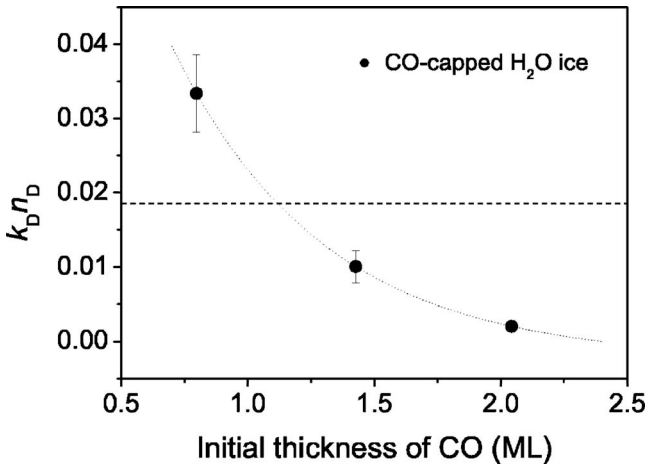

FIG. 4. Variation of the effective rate constant $k_D n_D$ with the amount of initial capped CO in the ice sample at 15 K. Solid circles represent the results for CO-capped H_2O ice samples. The horizontal dashed line gives fitting results of CO–H_2O mixed ice. The dotted line is included as a guide to the eye.

balance between the flux of the atoms, the sticking coefficient of the impinging atoms, and the loss of atoms by H–H (D–D) recombination. That is, the relation

$$S_i f - K_i [n_i]^2 = 0 \quad (i = \mathrm{H\ or\ D}), \tag{13}$$

is obtained, where the S_i and K_i are sticking coefficient and the rate constant of hydrogen recombination, respectively. Since H (D) atoms encounter immediately with each other before losing their initial kinetic energy (about 100 K) in the condition of high atom flux, the diffusion process would not be tunneling.[33] Therefore, the collision frequency is almost independent from the mass of atoms. Furthermore, H–H (D–D) recombination, namely, radical-radical reaction, is expected be the barrierless reaction. In fact, the potential energy surface for H_2 formation on graphite surface displays no energetic barrier.[34] As a result, the isotope effect on the rate constants of recombination must be negligible and thus the relation of those rate constants should be $K_H \simeq K_D$. Therefore, from Eq. (13), the ratio of n_D/n_H is expressed by

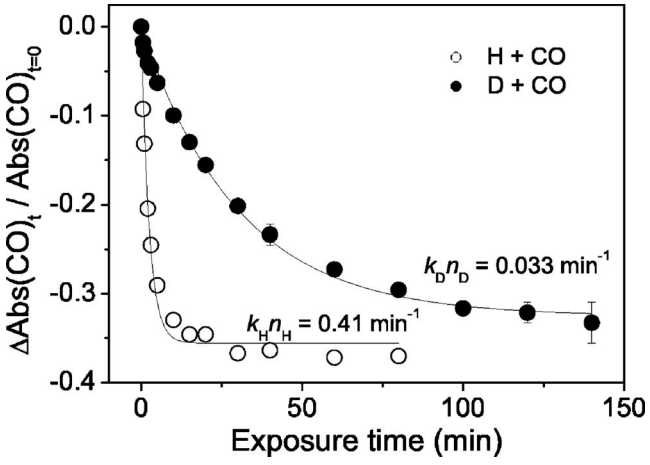

FIG. 5. Variation in absorbance of CO depletion after H (*open circle*) and D (*solid circle*) atom exposures of the CO-capped H_2O ice at 15 K. The solid lines are results of fitting using Eq. (12). The effective rate constants are obtained to be $k_H n_H = 0.41\ \mathrm{min}^{-1}$ and $k_D n_D = 0.033\ \mathrm{min}^{-1}$, respectively.

$$\frac{n_D}{n_H} = \sqrt{\frac{S_D}{S_H}}. \tag{14}$$

Since both D and H atoms are barely adsorbed on pure solid CO at 15 K [see, Fig. 2(a) and Ref. 12], the sticking coefficient to H_2O ice is responsible for those to the entire area of surface of the CO-capped H_2O ice at 15 K. Buch and Zhang[35] computationally studied the sticking processes of H and D atoms on amorphous ice (consisting of 115 water molecules) at 8–11 K. They found a simple formula of the sticking coefficient for an atomic temperature of $T \leqslant 300$K as follows:

$$S_i = (T/E_0 + 1)^{-2}, \tag{15}$$

where $E_0 = 102$ K for the H atom and $E_0 = 200$ K for the D atom. From this formula, the sticking coefficients of the H and D atoms on H_2O ice in the condition of the present experiments are 0.45 and 0.64, respectively. The calculated ratio of n_D/n_H from the sticking coefficients is about 1.2. Using molecular dynamics simulations, Masuda *et al.*[36] determined the sticking coefficient of H atoms to amorphous H_2O ice at 10 K to be 0.98–1. Although they did not calculate this for D atoms, the sticking coefficient of D atoms must be higher than that of the H atoms since the potential well of D–H_2O is deeper than that of H–H_2O. The results of Masuda *et al.* suggest that the sticking coefficient of D atoms to H_2O is almost unity, and thus the ratio of n_D/n_H becomes 1. Al-Halabi *et al.*[37] also investigated the sticking process of H atoms to the crystalline ice surface at 10 and 70 K. The sticking coefficient at 10 K is intermediate between that determined by Buch and Zhang[35] and Masuda *et al.*[36] There is no experimental work carried out for determining the sticking coefficients of H and D atoms on H_2O ice at very low temperatures. After all, it would be reasonable to consider that the n_D/n_H ratio is approximately unity. Using the relation of $n_D/n_H \sim 1$, the ratio of the reaction rate constant k_D/k_H is estimated to be about 0.08 in the present experiments. That is, CO+D→DCO DCO is 13 times slower than CO+H→HCO.

The reaction rate constant contains information on the activation energy of the chemical reaction. The available activation energy for CO+H(D) has been reported with a large variation (1000–7630 K) in literature.[13–17,38] Therefore, we attempted to estimate the activation barrier height by the analysis of experimental results with a model calculation of potential tunneling. The specific tunneling rate constant for a particle with energy E is described as $k(E) = \nu P(E)$, where $P(E)$ is the barrier permeability of the particle with a kinetic energy of E and ν is the frequency factor. The ratio of the frequency factors of D+CO and H+CO reactions (ν_D/ν_H) is expressed as an inverse ratio of the square root of the reduced mass. Using the asymmetrical Eckart potential for the activation barrier that is often adopted for reactions having large exothermicity,[39,40] the potential can be represented by

$$V(x) = -\frac{F_1 y}{1-y} - \frac{F_2 y}{(1-y)^2}, \tag{16}$$

$$y = -\exp(2x/d), \tag{17}$$

where x is the position in the reaction coordinate and d is the parameter of the barrier width. More precisely, d is a half-width at about half-height ($\Delta V_1/2.38$) of the symmetric Eckart potential. F_1 and F_2 can be represented by the potential barrier heights from the initial (ΔV_1) and the final (ΔV_2) states as follows:

$$F_1 = \Delta V_1 - \Delta V_2, \tag{18}$$

$$F_2 = \{(\Delta V_1)^{1/2} + (\Delta V_2)^{1/2}\}^2. \tag{19}$$

ΔV_1 and ΔV_2 can be replaced by E_a (the activation barrier height) and $E_a - \Delta H$ (ΔH: the heat of reaction), respectively. The exact expression for the barrier permeability of particles with energy E is given by

$$P_i(E) = \frac{\cosh\{2\pi(\alpha+\beta)\} - \cosh\{2\pi(\alpha-\beta)\}}{\cosh\{2\pi(\alpha+\beta)\} + \cosh 2\pi\delta} \quad (i = \text{H or D}), \tag{20}$$

where

$$\alpha = 1/2(E/F_3)^{1/2},$$

$$\beta = 1/2\{(E-F_1)/F_3\}^{1/2},$$

$$\delta = 1/2\{(F_2-F_3)/F_3\}^{1/2},$$

$$F_3 = \hbar^2/2\mu d^2, \tag{21}$$

and μ is the reduced mass. Finally, the ratio of the reaction rate constant of H to that for the D atom is written as

$$k_D/k_H = \nu_D/\nu_H \times P_D(E)/P_H(E). \tag{22}$$

The potential barrier profiles for CO+H and CO+D are slightly different because the zero-point energy of the activated complexes and products are different. That is, the shapes of the potentials are determined by $\Delta V_1 = E_a$ and $\Delta V_2 = E_a - \Delta H_{HCO}$ for the CO+H system, $\Delta V_1 = E_a - \Delta E_a$ and $\Delta V_2 = E_a - \Delta H_{DCO}$ for the CO+D system, where ΔE_a is the zero-point energy difference in the activated complex. The parameter of the barrier width d would have the same value for each reaction system because the shape of barrier is governed by the electron configuration. Thus, the ratio of reaction rate constants is represented as a function of the activation barrier height E_a and the parameter of the barrier width d. The barrier height of the H+CO reaction was derived theoretically by Werner *et al.*,[15] Woon,[13,14] Andersson and Grüning,[16] and Awad *et al.*,[38] and experimentally determined by Wang *et al.*[17] The calculated values are concentrated around 2000 K except for 7630 K as indicated by Awad *et al.*[38] The barrier height determined by the gas phase experiment is 1000 K,[17] which is significantly smaller than the calculated values. Consequently, using Eqs. (18)–(22) the ratio of the reaction rate constants was calculated at barrier heights of 1000, 2000, and 7630 K as a function of the barrier width parameter d in Fig. 6, and other parameters for the calculation are listed in Table I.

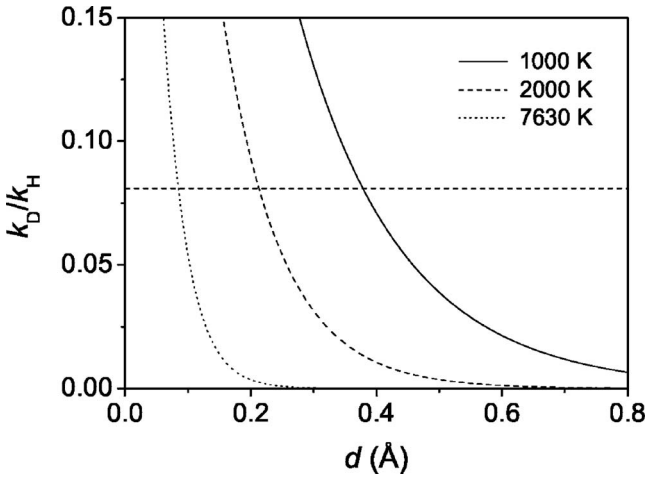

FIG. 6. The ratio of the rate constant for the isotopes k_D/k_H as a function of barrier width parameter d. Dotted, dashed, and solid lines are obtained from the calculation based on the tunneling of the asymmetrical Eckart potential with previously reported activation barrier heights E_a=1000, 2000, and 7630 K, respectively. The horizonal dashed line represents experimental results of the present study (see text).

The horizonal dashed line in Fig. 6 shows the value of $(k_D/k_H)_{expt}$ obtained in the present experiment. For barrier heights of 7630 and 1000 K, our obtained k_D/k_H ratio yields widths d of about 0.1 and 0.4 Å, respectively, which correspond to approximately 0.5–1.3 Å in the tunneling length of the asymmetrical Eckart potential at 15 K. The obtained widths seem small when compared to the common atomic distance in the neutral molecule. This may arise from the lower values of activation barrier heights in literature. All reported barrier heights are for gas phase reactions of H–CO (Refs. 13, 15, and 16) or H–CO–$(H_2O)_m$ ($m \leqslant 3$) (Ref. 14) systems and should be different from those at the surface. However, the transition probability is much more sensitive to the shape of the potential energy surface than the activation energy. Therefore, the choice of the Eckart potential can most likely be attributed to the narrow barrier width obtained. Nevertheless, the isotope effect on the ratio of the rate constants will be useful for the evaluation of the potential energy surface.

Finally, we mention another possibility for the CO depletion process, namely, $H_2+CO \rightarrow H_2CO$. In the gas phase, the activation energy of the above process was calculated to be 320.7 kJ/mol.[42] That is, this process is thermally allowed when the vibrational level of H_2 is larger than 8. The H_2 molecules are normally vibrationally pumped at the formation via the H–H recombination, because the heat of re-

TABLE I. Parameters used for the estimation of k_D/k_H with the asymmetric Eckart potential function.

Reaction	E (K)	ΔE_a (K)	ΔH (kJ/mol)
H+CO→HCO	15	···	−65.9[a]
D+CO→DCO	15	110[b]	−72.6[c]

[a]Experimental value in Ref. 41.
[b]The calculated zero-point energy correction at transition state between H–CO and D–CO in Ref. 14.
[c]This value calculated from −65.9 kJ/mol by using the zero-point energy correction of ΔE_{rxn} (net energy change of the reaction) (Ref. 14).

action is as large as 431.3 kJ/mol. The excited H_2 would desorb from the surface immediately upon formation by recombination. If the desorbed H_2 with $v \geqslant 8$ collide directly with the CO at the surface, the above process possibly occurs. It is suggested that the H_2 molecules experience multiple adsorption-desorption cycles or multiple collisions before being released to vacuum because of the irregular surface structure of amorphous ice.[33,43] The vibrational excited states of hydrogen molecules resulting from the recombination of atoms on a carbon surface were measured by Gough *et al.*[44] for surface temperatures of 90–300 K. In their experiments, the desorbed hydrogen molecules were detected up to $v=7$ with a population of about 10^{-5} from $v=7$ to $v=0$. Although the vibrational population of H_2 pumped by recombination on amorphous ice has not been reported, a similar distribution of vibrational states on amorphous ice would be expected because of the small difference in binding energy between H–amorphous ice[35] and H–graphite[45] compared with the energy-level spacing of vibrational states in H_2. In our experiments, one CO molecule was consumed per approximately several hundreds of hydrogen atoms. Therefore, the reaction $H_2+CO \rightarrow H_2CO$ is unlikely because of the small relative population of $H_2(v=7)/H_2(v=0) \sim 10^{-5}$.

IV. ASTROPHYSICAL IMPLICATION

In interstellar molecular clouds, deuterated formaldehyde and methanol molecules have been found with relative abundances (e.g., CH_3OH-d/CH_3OH) of up to 0.65 with reference to the normal molecules.[46] Since normal H_2CO and CH_3OH can be produced by the successive hydrogenation of CO on the dust surfaces, deuterated species may be produced by the deuteration. However, considering the obtained ratio of $(k_D/k_H)_{expt} \simeq 0.1$ and the D/H atom ratio of 0.1 or less[47] expected in molecular clouds, deuterium addition to CO is not favorable as the first step to produce deuterated formaldehyde and methanol, especially since D_2CO and CD_3OH have been observed abundantly in molecular clouds. Obviously, other processes such as the H–D substitution reaction in formaldehyde and methanol suggested by Nagaoka *et al.*[19] are necessary to achieve the observed abundances of the deuterated species. The present results also show that the reaction rates strongly depend not only on the surface temperatures but also on the composition and structure of the ice surface. For instance, although the deuteration of CO on solid CO ice only proceeds at 10 K, those on CO-capped H_2O and $CO-H_2O$ mixed ice proceed up to 20 K. The reaction rates also vary with the amount of CO on the ice surface. These facts indicate that modeling including the temperature and composition of interstellar ice is very important for the study of chemical evolution in space.

V. CONCLUSIONS

We performed experiments on D atom exposure of three types of ice samples (solid CO, CO-capped H_2O, and $CO-H_2O$ mixed) at 10–20 K. The successive addition of D atoms to CO to produce D_2CO and CD_3OD was observed. The reaction rate of D+CO strongly depends not only on the surface temperature but also on the composition of the sample. The effective rate constants decrease with increasing CO coverage at the surface. In other words, the presence of H_2O molecules at the surface enhances the effective rate constants and raises the reactive temperature. This may be due to the higher sticking coefficient of atoms to H_2O ice than pure solid CO. Alternately, H_2O ice may act as a catalyst.

The isotope effect in the reaction rates for H(D)+CO on CO-capped H_2O ice was investigated. The ratio of the reaction rate constant k_D/k_H is about 0.08 at 15 K. The obtained ratio in the present experiments provides useful information for the potential energy surface of the H+CO reaction on the surface of ice.

ACKNOWLEDGMENTS

This work was supported in part by a Grant-in-Aid for Scientific Research from the Japan Society for the Promotion of Science and the Ministry of Education, Science, Sports, and Culture of Japan.

[1] T. Kumada, K. Komaguchi, Y. Aratono, and T. Miyazaki, Chem. Phys. Lett. **261**, 463 (1996).
[2] H. Tsuruta, T. Miyazaki, K. Fueki, and N. Azuma, J. Chem. Phys. **87**, 5422 (1983).
[3] T. Miyazaki, K.-P. Lee, K. Fueki, and A. Takeuchi, J. Chem. Phys. **88**, 4959 (1984).
[4] H. Hoshina, M. Fushitani, and T. Momose, J. Chem. Phys. **120**, 3706 (2004).
[5] E. D. Sprague and F. Williams, J. Am. Chem. Soc. **93**, 787 (1971).
[6] E. L. Gibb, D. C. B. Whittet, A. C. A. Boogert, and A. G. G. M. Tielens, Astrophys. J., Suppl. **151**, 35 (2004).
[7] A. G. G. M. Tielens and W. Hagen, Astron. Astrophys. **114**, 245 (1982).
[8] K. Hiraoka, T. Sato, S. Sato, N. Sogoshi, T. Yokoyama, H. Takashima, and S. Kitagawa, Astrophys. J. **577**, 265 (2002).
[9] N. Watanabe and A. Kouchi, Astrophys. J. Lett. **571**, L173 (2002).
[10] N. Watanabe, T. Shiraki, and A. Kouchi, Astrophys. J. Lett. **588**, L121 (2003).
[11] H. Hidaka, N. Watanabe, T. Shiraki, A. Nagaoka, and A. Kouchi, Astrophys. J. **614**, 1124 (2004).
[12] N. Watanabe, A. Nagaoka, T. Shiraki, and A. Kouchi, Astrophys. J. **616**, 638 (2004).
[13] D. E. Woon, J. Chem. Phys. **105**, 9921 (1996).
[14] D. E. Woon, Astrophys. J. **569**, 541 (2002).
[15] H. J. Werner, C. Bauer, P. Rosmus, H. M. Keller, M. Stumpf, and R. Schinke, J. Chem. Phys. **102**, 3593 (1995).
[16] S. Andersson and M. Grüning, J. Phys. Chem. A **108**, 7621 (2004).
[17] H. Y. Wang, J. A. Eyre, and L. M. Dorfman, J. Chem. Phys. **59**, 5199 (1973).
[18] H. B. Xie, Y. H. Ding, and C. C. Sun, Astrophys. J. **643**, 573 (2006).
[19] A. Nagaoka, N. Watabnabe, and A. Kouchi, Astrophys. J. Lett. **624**, L29 (2005).
[20] N. Watanabe, A. Nagaoka, H. Hidaka, T. Shiraki, T. Chigai, and A. Kouchi, Planet. Space Sci. **54**, 1107 (2006).
[21] G. J. Jiang, W. B. Person, and K. G. Brown, J. Chem. Phys. **64**, 1201 (1975).
[22] W. Hagen, A. G. G. M. Tielens, and J. M. Greenberg, Chem. Phys. **56**, 367 (1981).
[23] N. Koch and E. Steffens, Rev. Sci. Instrum. **70**, 1631 (1999).
[24] T. Tso and E. K. C. Lee, J. Phys. Chem. **88**, 5475 (1984).
[25] M. Falk and E. Whalley, J. Chem. Phys. **34**, 1554 (1961).
[26] D. E. Milligan and M. E. Jacox, J. Chem. Phys. **41**, 3032 (1964).
[27] D. E. Milligan and M. E. Jacox, J. Chem. Phys. **51**, 277 (1969).
[28] M. E. Jacox and D. E. Milligan, J. Mol. Spectrosc. **47**, 148 (1973).
[29] M. E. Jacox, Chem. Phys. **59**, 213 (1981).
[30] G. Inoue, H. Akimoto, and M. Okuda, J. Phys. Chem. **72**, 1769 (1980).
[31] B. Kerkeni and D. C. Clary, Phys. Chem. Chem. Phys. **8**, 917 (2006).
[32] L. Hornekær, A. Baurichter, V. V. Petrunin, D. Field, and A. C. Luntz,

Science **302**, 1943 (2003).
[33] H. B. Perets, O. Biham, G. Manicó, V. Pirronello, J. Roser, S. Swords, and G. Vidali, Astrophys. J. **627**, 850 (2005).
[34] A. J. Farebrother, A. J. H. M. Meijer, D. C. Clary, and A. J. Fisher, Chem. Phys. Lett. **319**, 303 (2000).
[35] V. Buch and Q. Zhang, Astrophys. J. **379**, 647 (1991).
[36] K. Masuda, J. Takahashi, and T. Mukai, Astron. Astrophys. **330**, 773 (1998).
[37] A. Al-Halabi, A. W. Kleyn, E. F. van Dishoeck, and G. K. Kroes, J. Phys. Chem. B **106**, 6515 (2002).
[38] Z. Awad, T. Chigai, Y. Kimura, O. M. Shalabiea, and T. Yamamoto, Astrophys. J. **626**, 262 (2005).
[39] C. Eckart, Phys. Rev. **35**, 1303 (1930).
[40] H. S. Johnston and J. Heicklen, J. Phys. Chem. **66**, 532 (1962).
[41] M.-C. Chuang, M. F. Foltz, and C. B. Moore, J. Chem. Phys. **87**, 3855 (1987).
[42] K. Ohno and S. Maeda, J. Phys. Chem. A **110**, 8933 (2006).
[43] S. Morisset, F. Aguillon, M. Sizun, and V. Sidis, J. Chem. Phys. **122**, 194702 (2005).
[44] S. Gough, C. Schermann, F. Pichou, M. Landau, I. Čadež, and R. I. Hall, Astron. Astrophys. **305**, 687 (1996).
[45] E. Ghio, L. Mattera, C. Salvo, F. Tommasini, and U. Valbusa, J. Chem. Phys. **73**, 556 (1980).
[46] B. Parise, C. Ceccarelli, A. G. G. M. Tielens, A. Castests, E. Caux, B. Lefloch, and S. Maret, Astron. Astrophys. **453**, 949 (2006).
[47] H. Robert, E. Herbst, and T. J. Millar, Mon. Not. R. Astron. Soc. **336**, 283 (2002).